

Research on preview control algorithm of PRS-XY hybrid machine tool based on kinematics calculation

Lina Li¹, Hongchang Sun^{2,*}, and Zhigang Niu³

¹Department of Automobile Engineering, Tianjin Transportation Vocational College, Tianjin, China

²Institute of Robotics and Intelligent Equipment, Tianjin University of Technology and Education, Tianjin, China

³School of Mechanical Engineering, Tai Yuan University of Technology, Tai Yuan, Shanxi, China

Abstract. This paper presents a preview control algorithm (PCA) for hybrid machine tool based on kinematics calculation. HMT (Hybrid Machine Tool) combines the flexibility of parallel structure with the extensibility of series structures. The kinematics are calculated and analyzed as well as the calculation process. Due to the complexity of its structure and kinematics algorithms, a motor PCA is proposed in the situation of calculation failure and used to reduce the corresponding motor vibration. The experimental results shows that the PCA is an effective way to detect and suppress the motor vibration and shock during the motion control of PRS-XY HMT.

Keywords: PRS-XY HMT, Kinematics, Vibration suppression, Preview control algorithm.

1 Introduction

At present, more and more research productions have achieved on the Serial-Parallel mechanism [1-2].

The use of three parallel mechanism were all taken the three-bar parallel mechanism as their main machine tool structures. In order to achieve the high control performance of the hybrid machine tool, it is necessary to give the perfect control method based on the kinematic calculation of the PRS-XY HMT. Based on the perturbation observer control method, the higher gain achieves better control performance, but for the linear motor servo system without any intermediate buffer link, excessive gain is not conducive to system stability[3]. Here is a robust control based on the control method, mainly by suppressing the vibration of the cutting process to achieve good control performance[4]. Based on the online learning control method, the shortcomings of its slow convergence speed is not conducive to the realization of high-speed and stable motion control[5]. Preview control

* Corresponding author: sunhongchang@tute.edu.cn

can be based on a linear control object model, or based on a nonlinear control object model, but requires precise control of the object model [6].

2 Structural characteristics and kinematic analysis of PRS-XY HMT

2.1 The coordinate system configuration for PRS-XY HMT.

The reference coordinate system $O_2-X_2Y_2Z$ is established on the X-Y table and its initial position is completely coincident with the absolute coordinate system (or fixed coordinate system) $O-XYZ$. The inverse kinematics analysis can be described as the calculations from the known tool tip positions and the axial attitude parameters, to the unknown S_1, S_2, S_3, X and Y . So the known condition is the position of the tool tip $(x_t, y_t, z_t)^T$, tool tip position (x_t^e, y_t^e, z_t^e) within the coordinate system $O_2-X_2Y_2Z_2$ and the direction vector of the axis $N_t=(n_{tx}, n_{ty}, n_{tz})^T$. PRS-XY coordinate system configuration and the real machine shown in Fig. 1.

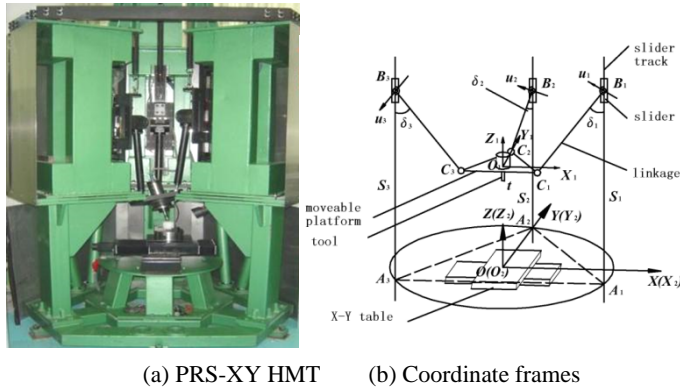


Fig. 1. PRS-XY HMT object and its Coordinate frames.

2.2 Inverse kinematics analysis and calculation for PRS-XY HMT.

Due to the particularity of the parallel structure, the kinematic calculation becomes more important when there is a nonlinear relationship between the tool tip coordinates and the joint coordinates, so the application of preview control in these areas, especially with kinematic participation in the motion control is of great significance. are listed as bellow[7]:

The result was given from reference [8] :

$$\begin{cases} S_1 = \sqrt{L^2 - \left(\frac{\sqrt{3}}{2}R - \frac{\sqrt{3}}{2}rl_x + \frac{3}{2}rm_x\right)^2 - \left(-\frac{1}{2}R - \frac{\sqrt{3}}{2}rl_y + \frac{1}{2}rl_x\right)^2} + \frac{\sqrt{3}}{2}rl_z - \frac{1}{2}rm_z + z_c \\ S_2 = \sqrt{L^2 - \left(R + \frac{1}{2}rl_x - \frac{3}{2}rm_y\right)^2} + rm_z + z_c \\ S_3 = \sqrt{L^2 - \left(-\frac{\sqrt{3}}{2}R + \frac{\sqrt{3}}{2}rl_x + \frac{3}{2}rm_x\right)^2 - \left(-\frac{1}{2}R + \frac{\sqrt{3}}{2}rl_y + \frac{1}{2}rl_x\right)^2} - \frac{\sqrt{3}}{2}rl_z - \frac{1}{2}rm_z + z_c \end{cases} \quad (1)$$

$$\begin{cases} x_{o2} = x_t - x_t^e \\ y_{o2} = y_t - y_t^e \end{cases} \quad (2)$$

During the machining, the changes of tool attitude are formed by the rotation of A and B axes. Due to the independence of the A, B axis movement, the motion of any axis does not

affect the coordinate values of the other axis. Make the *B*-axis rotation angle or coordinate value be *b*, that is, the angle of the projection of the arbor in the *XO₁Z* plane and the angle of the *Z*-axis; the *A*-axis rotation angle or coordinate value is *a*, that is, the angle between the arbor and its projection in the *XO₁Z* plane. Obviously, the tool posture is uniquely determined by *a*, *b*. (*x_{t1}*, *y_{t1}*, *z_{t1}*), according to the cosine angle to calculate the coordinates of the tip point *P_{t1}*: (*r cos θ_x*, *r cos θ_y*, *r cos θ_z*). According to *A*, *B* axis angle and *b* to guide the coordinates of the tip point *P_{t1}*, combined with the Fig. 1, it can be obtained as[7]:

$$\begin{cases} r \cos a \sin(-b) = r \cos \theta_x \\ r \sin a = r \cos \theta_y \\ -r \cos a \cos(-b) = r \cos \theta_z \end{cases} \quad (3)$$

From Eq.3, Eq.4 is also available:

$$\begin{cases} a = \arcsin \cos \theta_y \\ b = -\arcsin \frac{\cos \theta_x}{\sin \theta_y} \end{cases} \quad (4)$$

Make $S_4 = x_{o_2}$, $S_5 = y_{o_2}$, $x = x_t^e$, $y = y_t^e$, $z = z_t^e$, so inverse kinematic transformation can be simplified as:

$$S_i = f_i(x, y, z, a, b) \quad i = 1, 2, 3, 4, 5 \quad (5)$$

From the Eq.5, the hybrid machine programming method can be implemented as same as the conventional programming within Cartesian coordinate system: *X*, *Y*, *Z*, *A*, *B*, and five-axis machining can be achieved by the inverse kinematic calculation.

2.3 Direct kinematics analysis and calculation for PRS-XY HMT.

From Fig.1, $\Delta\theta_1, \Delta\theta_2, \Delta\theta_3$ are angles between standard angle (120°) and OA_1, OA_2, OA_3 . C_1, C_2 and C_3 meet the following constraint conditions, for they are just as long as the sides of the equilateral triangle[9].

$$\begin{cases} \left[-\frac{1}{2}(R - L\sin\delta_2) + \frac{1}{2}(R - L\sin\delta_3) \right]^2 + \left[\frac{\sqrt{3}}{2}(R - L\sin\delta_2) + \frac{\sqrt{3}}{2}(R - L\sin\delta_3) \right]^2 + (S_2 - L\cos\delta_2 - S_3 + L\cos\delta_3)^2 = 3r^2 \\ \left[R - L\sin\delta_1 + \frac{1}{2}(R - L\sin\delta_3) \right]^2 + \left[0 + \frac{\sqrt{3}}{2}(R - L\sin\delta_3) \right]^2 + (S_1 - L\cos\delta_1 - S_3 + L\cos\delta_3)^2 = 3r^2 \\ \left[R - L\sin\delta_1 + \frac{1}{2}(R - L\sin\delta_2) \right]^2 + \left[0 - \frac{\sqrt{3}}{2}(R - L\sin\delta_2) \right]^2 + (S_1 - L\cos\delta_1 - S_2 + L\cos\delta_2)^2 = 3r^2 \end{cases} \quad (6)$$

C_1, C_2, C_3 should satisfy the following constraints[9]:

$$\left| \overline{C_1 C_2} \right|^2 = \left| \overline{C_2 C_3} \right|^2 = \left| \overline{C_1 C_3} \right|^2 = 3r^2 \quad (7)$$

The results can be concluded from reference[18], the posture equation for the machine, and the standardized equation is[8]:

$$Y = Y_1^2(\delta_1, \delta_1) + Y_2^2(\delta_2, \delta_3) + Y_3^3(\delta_3, \delta_1) \quad (8)$$

3 Analysis on the vibration principle of hybrid machine tool

During the motion control of the hybrid machine tool, for the direct kinematics, once the kinematic calculation is overtime or the position of the real axis motor has not been

subjected to inverse kinematics, The impact of the machine, the machine vibration, will make the actual position of the tool and the calculation of the location does not match to each other, so that control errors, which will lead to uncontrolled movement, and then the impact of vibration and other phenomena will arise.

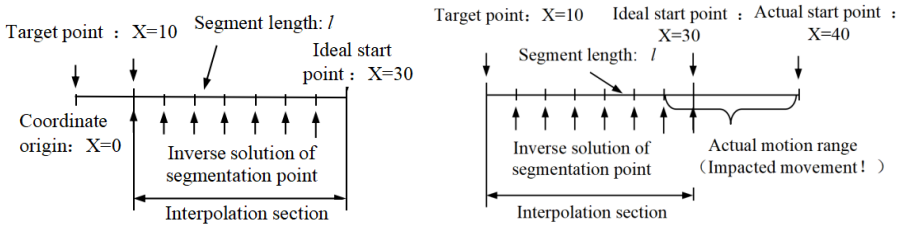


Fig. 2. The ideal Kinematic control process.

Fig. 3. The misplaced Kinematic control process.

The cause of this error is illustrated by Fig.2 to Fig.3. "G01X10", the instructions for the implementation of the process is given as an example in Fig 3. When the real axis motor is manually moved by 10 mm to simulation the situation that the inverse kinematics solution is not given properly by kinematic program. When the starting point of the tool tip is determined by the direct kinematic calculation procedure, it is still the coordinate value before the tool tip movement, resulting in the actual starting position of the tool tip deviation from the calculation of the starting point of 10mm.The trajectory planning interpolation is performed on the virtual axis and the position $X= 30\text{mm}$ is used as the starting point of the trajectory interpolation to plot the given target $X=10\text{mm}$ as the interpolation end point, the interpolation period is T , the segment length is l . When moving control, it is required to move l length in T time. In fact, it is necessary to move $(10+l)$ mm in the first interpolation cycle T . Assuming that the feed rate is $F = 1000\text{mm} / \text{min}$ and the interpolation period $T = 10\text{ms}$, the planned segmentation movement amount is set to 0.167mm according to the interpolation formula in the Turbo PMAC[10], and the actual movement amount is 10.167 mm, about 60 times the planned movement. This vibration will continue to the subsequent interpolation cycle, until the actual position and the calculation of the same position when the movement tends to normal, resulting in impact movement of PRS-XY HMT .

4 Impact suppression strategy based on preview control

In order to overcome the impact, one of the effective ways is to include preview control in the control loop. The preview control system based on feedforward compensation consists of a basic control loop and a preview feedforward loop. In order to reduce the overshoot and enhance the suppression ability to the load disturbance, The I-P control loop is used as the basic circuit of control circuit[11]. Based on this, preview feedforward compensation link is added to form the preview feed forward control . In the basic circuit of preview control, set the impact be the interference error signal, and state feedback is implemented in its error systemlike this:[13-14].

$$\Delta u(k) = F_1 X_0(k) \tag{9}$$

To constitute a stable control system, and F_1 can be based on the principle of optimal feedback design. Make $F_1 = [F_e \quad F_x]$, and

$$\Delta u(k) = F_1 X_0(k) = [F_e \quad F_x] \begin{bmatrix} e(k) \\ \Delta x(k) \end{bmatrix} = F_e e(k) + F_x \Delta x(k) \tag{10}$$

Solve the value of $u(k)$ from the above equation $u(k)$, then:

$$u(k) = F_e \sum_{j=1}^k e(j) + F_x x(k) - F_x x(0) + u(0) \tag{11}$$

Let the initial state be zero, then:

$$u(k) = F_e \frac{1}{1-z^{-1}} e(k) + F_x x(k) \tag{12}$$

It is now assumed that the target signal from the current moment k to the future M_R step and the interference signal to the next M_d step are known. The structure of the preview control system using these signals is shown in Fig.4.

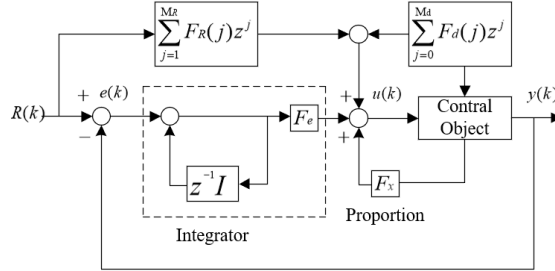


Fig. 4. Preview feed forward compensation system structure.

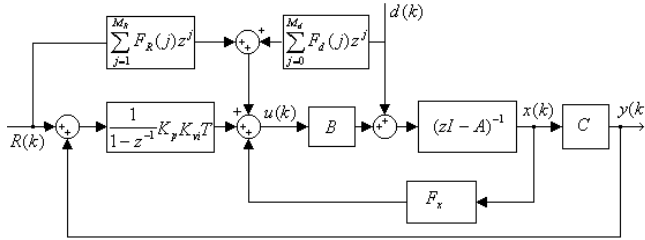


Fig. 5. Preview control block diagram.

For the motion controller Turbo PMAC, The results of the kinematic calculation and the impact motion of the linear motor are added to the control input as a system input and a dynamic disturbance component, respectively, resulting in an unpredictable control effect on the output. In Fig.4, the input increment for the preview control is:

$$\Delta u(k) = F_1 X_0(k) + \sum_{j=0}^{M_R} F_{1R}(j) \Delta R(k+j) + \sum_{j=0}^{M_d} F_d(j) \Delta d(k+j) \tag{13}$$

Where $F_{1R}(j)$ and $F_d(j)$ are the target feedback coefficients to be determined and the interference feedforward coefficients.

By transformation:

$$u(k) = \sum_{j=0}^{M_R} F_{1R}(j) R(k+j) + \sum_{j=0}^{M_d} F_d(j) d(k+j) + F_1 \left[\frac{1}{1-z^{-1}} e(k) \quad x(k) \right] \tag{14}$$

Set the control object model to:

$$H(z) = \frac{b_1 z^{-1} + b_2 z^{-2} + b_3 z^{-3}}{1 + a_1 z^{-1} + a_2 z^{-2} + a_3 z^{-3}} \tag{15}$$

According to the linear discrete time system, the following conclusions can be drawn:

$$\begin{cases} x(k+1) = Ax(k) + Bu(k) \\ y(k) = Cx(k) + Du(k) \end{cases} \tag{16}$$

In general, the system direct transfer matrix $D=0$, so the linear discrete-time system is generally described as:

$$x(k) = (zI - A)^{-1} Bu(k) \tag{17}$$

Among them, the state equation coefficient matrix is equivalent to:

$$A = \begin{bmatrix} 0 & 0 & -a_3 & 0 \\ 1 & 0 & -a_2 & 0 \\ 0 & 1 & -a_1 & 0 \\ 0 & 0 & 1 & 0 \end{bmatrix} \quad B = \begin{bmatrix} b_3 \\ b_2 \\ b_1 \\ 0 \end{bmatrix} \quad C = [0 \ 0 \ 1 \ 0] \quad D = 0 \tag{18}$$

Transform the equivalent control loop and superimposed preview feed forward items in Fig4. Furthermore, the complete preview control structure is shown in Fig 5, which is going to be written to Turbo PMAC as a preview control algorithm.

5 Experiment and analysis of vibration suppression

For clear observation and analysis, the virtual axis coordinates are converted to the real axis by 1: 1 by the kinematic program. Therefore, the length of the fine interpolation section on the real axis motor is 0.033mm. As shown in Fi.6, move the motor -0.5mm manually, thus changing the motor starting point. The actual length of the first interpolation cycle $l' = 0.533\text{mm}$, about 16 times the normal amount of exercise, the real axis of the total movement of 10.5mm. In this way, a more severe variation is constructed, which is the case when the direct kinematic model is calculated without a solution or a calculation error due to a deviation in the starting point of the movement and without taking corrective action. When the NC program is running, a data graph with a sampling period of 50ms.

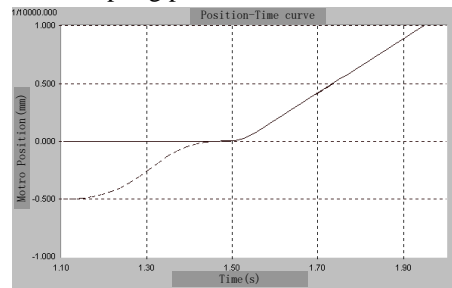
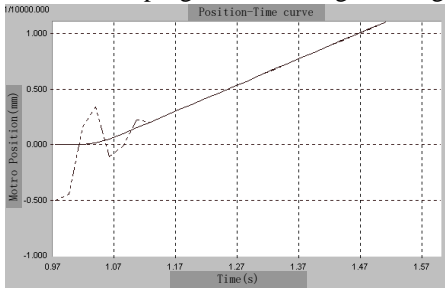


Fig. 6. Position-Time curve without PCA involved. **Fig. 7.** Position-Time curve with PCA.

As can be seen from Fig.6, at the point of variation, the X motor oscillates due to the high acceleration, which oscillates for about 0.16 s. And the Y motor has been moving at a given interpolated cycle, since the X motor oscillation state maintains a plurality of interpolation periods, making the motion synthesis trajectory off the programming trajectory. It can be seen from Fig. 7, under the action of the preview control algorithm, X motor in the variation without oscillation, about 0.4s after the movement tends to normal. While the Y motor in the period of displacement only a very small amount of change, apparently did not enter the next interpolation cycle. This makes it very clear that the preview control algorithm extends the interpolation period so that the run time of all the motors in the same motion block is synchronized at the point of variation, although some motors do not appear abnormal. It will suppress the motor oscillation, but also the synthesis of motion does not deviate from the programming trajectory, to ensure the processing accuracy, and be able to meet the restrictions on motor movement, which can effectively inhibit the motor vibration, protect the motor and the machine structures.

6 Summary

Due to the special structure and control methods, it is easy to produce the impact and vibration of the motor, especially in the case of singular solution of kinematics happened. In order to overcome this situation, the cause and hazard of the shock and vibration of the motor were analyzed. This paper also introduces a kind of kinematic based preview control algorithm which is analyzing its kinematic characteristics and machine motion control mechanisms, and in limiting motor speed and acceleration. Preview control algorithm's ability to suppress abnormal vibration and shock was verified by experiment. This paper pointed out that for the hybrid machine tool, whose motion control was based on kinematic calculation, is able to work well under the preview control algorithm.

This paper is supported by TUTE Science and Technology Development Fund (KJ2003).

References

1. Sun, H. , Yi, D. , Zhang, J. , & Li, L. . (2010). Simulation and numerical analysis based on kinematics of PRS-XY Serial-Parallel PKM. *IEEE* (Vol.4, pp.1531-1536). IEEE.
2. Chu Kaiyu. *New CNC machine tool in the 21st Century- Virtual Axis Machine Tool* [J]. Mechanical Engineer, 2014, 8: 15-17
3. Stoelen, M. F. , et al. Measuring Progress on an Approach for Interactive Learning of Context-Driven Actions. 2020.
4. Patan, K. , & Patan, M. . (2020). Neural-network-based iterative learning control of nonlinear systems. *ISA Transactions*, 98, 445-453.
5. Qi c, Neural network control theory [M], Northwestern Polytechnical University Press, 2000
6. Liang, M. , Wu, X. , Wang, Y. , Zhu, Z. , & J Xu. (2021). Multi-model and multi-expert correlation filter for high-speed tracking. *IEEE Access*, PP(99), 1-1.
7. Sun H , Zhang Z A , Jin X A , et al. Research on Virtual-real Biaxial Real-time Error Compensation Based on Fuzzy Control Theory[J]. *Procedia CIRP*, 2018, 76:115-120.
8. Sun Hongchang etc., The Research of Numerical Control Transformation Based on Turbo PMAC, 2014 (Volumes 989 - 994), 3240-3243
9. Niu Z , Ming L . Kinematics Analysis for a New-Style Machine Tool Based on 3-PRS Parallel Robot[C]// *International Conference on Intelligent Robotics and Applications*. Springer, Berlin, Heidelberg, 2008.
10. Delta Tau Data System Inc. *Open Servo User's Manual*. Chatsworth, USA: Delta Tau Data System Inc, 2021
11. Herrera-Granda I D , Lorente-Leyva L L , DH Peluffo-Ordóez, et al. A Forecasting Model to Predict the Demand of Roses in an Ecuadorian Small Business Under Uncertain Scenarios[M]. 2020.
12. Li Y , Zhao M , Zhou S . Servo axis incipient degradation assessment of CNC machine tools using the built-in encoder[J]. *International Journal of Advanced Manufacturing Technology*, 2020, 106(4).
13. Chen J . Sliding Mode Preview Control for a Class of Continuous-Time Linear Systems[J]. *Iranian Journal of Science and Technology - Transactions of Electrical Engineering*, 2020, 44(1).

14. Xiang-Ru L I , Gen-Suo MI . Research on Speed Controller of High-Speed Train Based on Optimal Preview Control[J]. *Measurement & Control Technology*, 2019.